Experimental Investigation of Pilot Dynamics in a Pilot-Induced Oscillation Situation

D. L. HIRSCH* AND R. L. MCCORMICK†
Northrop Corporation, Hawthorne Calif.

Results are presented for an experimental fixed and moving-base flight simulator investigation of a generalized aircraft longitudinal pilot induced oscillation (PIO) situation. Data are given relative to four handling-quality areas 1) pilot dynamic performance when tracking sinusoidal inputs following the occurrence of PIO, 2) the influence of motion cues on such performance, 3) the effects of varying stick force on pilot dynamic behavior in the PIO situation, and 4) the effect of varying the vehicle short-period transfer function numerator term $1/T_{\theta_2}$. Increases in this term to values above the normal level associated with the simulated airframe yielded experimental PIO's. The intentional increases were accomplished at a high input rate in an effort to preclude significant initial pilot gain adaptation. Approximately five times the increase in $1/T_{\theta_2}$ which produced the moving-base PIO was needed to produce instances of fixed-base PIO. With only external visual cues available during an oscillation, the pilot did not appear to operate in a synchronous (pure gain) manner. The availability of full-scale motion cues with visual cues causes the pilot to appear more nearly synchronous in the visual loop; however, the same data more consistently show the pilot operating with lag dynamics on the load factor cues.

Nomenclature

a_{z} = normal acceleration at the pilot's location, g's
F_p = stick force, lb
g = acceleration due to gravity, ft/sec^2
j = $(-1)^{1/2}$
$j\omega$ = imaginary portion of complex variable, $\sigma + j\omega$
K_c = control gain, deg δ_H/lb F_p
K_F = stick force gradient at stick grip, lb/in.
K_p = pilot gain, lb F_p/deg θ_ϵ
K_{wsp} = gain of vertical velocity short-period transfer function, ft/deg δ_H
$K^{*}_{\theta_{sp}}$ = gain of pitch attitude short-period transfer function, deg θ/deg δ_H
M_q = pitching acceleration per unit pitching velocity, 1/sec
M_w = pitching acceleration per unit vertical velocity, 1/sec-ft
$M_{\dot{\alpha}}$ = pitching acceleration per unit rate of change of angle of attack, 1/sec
M_δ = pitching acceleration per unit horizontal tail deflection, 1/sec^2
q = pitching angular velocity, rad/sec
s = laplace transform operator
$1/T_{w1}$ = vertical velocity numerator inverse time constant, 1/sec
$1/T_{\theta_2}$ = pitch attitude numerator inverse time constant, 1/sec
u_0 = forward-velocity/57.3, fps
w = airframe perturbed velocity along vertical axis, fps
Z_δ = vertical acceleration per unit horizontal tail deflection, ft/sec^2-rad
δ_H = horizontal tail deflection, deg
δ_s = stick grip deflection, in.
ζ_{sp} = airframe short-period damping ratio
θ_f = perturbation airframe pitch angle; simulator cab pitch angle, deg
σ = real portion of complex variable, $\sigma + j\omega$
ω_{sp} = airframe short-period natural frequency, rad/sec

Subscripts

B = simulator beam
C = simulator cab
c = control
F = stick force
g = gust
H = horizontal tail
hor = horizon
i = input
o = output
p = pilot
s = stick
sp = short period
W = vertical velocity
z = vertical axis
$\dot{\alpha}$ = angle of attack angular velocity
ϵ = error
θ = pitch angle

Presented as Preprint 65-793 at the AIAA/RAeS/JSASS Aircraft Design and Technology Meeting, Los Angeles, Calif., November 15–18, 1965; submitted December 7, 1965; revision received June 30, 1966.

* Member of Technical Management. Member AIAA.
† Senior Engineer, Norair Division. Member AIAA.

Introduction

As a result of recent experimental and theoretical handling-quality investigations,[1,2] there has arisen legitimate debate as to the cause of pilot-induced oscillations in contemporary aircraft, and satisfactory criteria to offset them. Central and necessary to the evolution of such criteria is a knowledge of the dynamic behavior of the pilot during the PIO situation. A review of rare but sometimes available flight time histories of PIO's (of which Fig. 1 is an example) reveals three distinct and differing periods of total system behavior. Analyses of PIO difficulties on specific airframes have also been undertaken.[3,4] Prior to the PIO, the pilot-control-airframe system exhibits a normal tracking behavior where the pilot is most often controlling random-appearing inputs. The last period is the developed PIO where the apparent airframe motions are of a nearly sinusoidal form. Between the pre-PIO and developed-PIO periods is a transient period that contains the time-varying excitation, vehicle, control, and pilot changes which serve to initiate the PIO. Random-appearing system behavior has been the subject of exhaustive analytical and experimental efforts, and theoretical pilot models applicable to this phase are available to the handling-quality analyst; however, by its very nature, the period of developed PIO has not been amenable to generalized analysis. In fact, an advance in the state-of-art of ground-based flight simulators was necessary before comprehensive experimental investigation of this phase could be undertaken. With this capability, the intent of the investigation reported herein was to produce an experimental evaluation of pilot dynamics in the developed-PIO phase. It is hoped that continued research with these data will yield a pilot model and thereby equip the handling-quality analyst with powerful theoretical tools for PIO prognosis or preven-

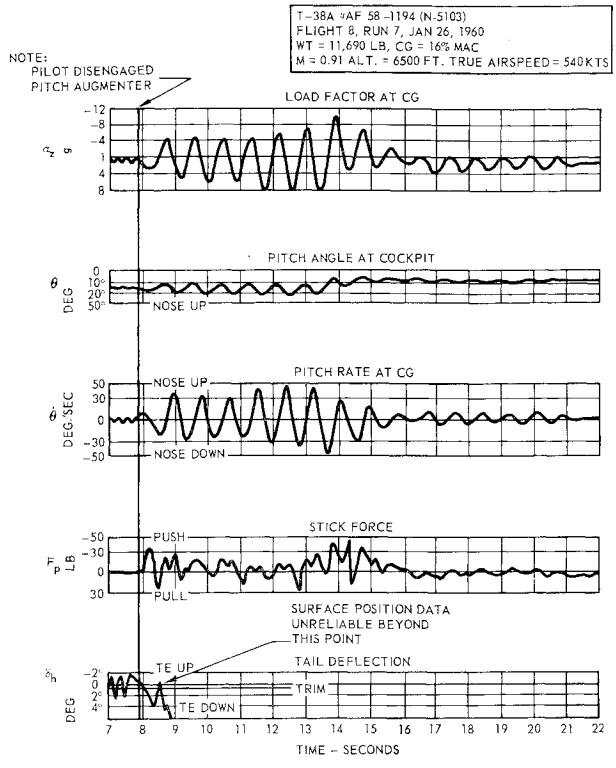

Fig. 1 Time history of a PIO.

tion in new aircraft designs. Ultimately, a detailed analysis of the transient (or mid-PIO) phase of pilot dynamics will have to be undertaken before final agreed-upon criteria for PIO prevention evolve; however, the transient period, which was intentionally induced by an airframe dynamics change in the course of these experiments, has not been the subject of analysis in this evaluation. Subjective evaluation of this period still appears to require an advance in the knowledge concerning pilot time-varying characteristics.

The reader is again reminded that the nature of this investigation is experimental. An analysis has not been undertaken which would test enough theoretical pilot transfer function possibilities to select one finally for the developed PIO phase. Such an effort is a needed and logical sequel to conclude this investigation.

The Experiment

A pilot was placed in the simulated pitch control loop representative of a conventional jet fighter aircraft flying under visual conditions in moderate turbulence at low altitude and high speed. Only the pitch axis could be controlled by the pilot; lateral and directional degrees of freedom were held fixed. To obtain the "tightness" of pilot control representative of actual precision flight tasks conducive to PIO, the simulator flight task was reduced to one of pure compensatory tracking in pitch. The pilot viewed a horizon external to the cockpit with display sensitivity analogous to the "real world" situation. An input gust disturbance of known frequency and amplitude was applied to the airframe and the pilot was instructed to track the horizon. Following a normal 2- to 4-min tracking exposure, and without warning to the pilot, the value of $1/T_{\theta_2}$ in the vehicle transfer function numerator was rapidly increased. Airframe gain, control system gain, and airframe short period and damping were all left unaltered. The experiment was terminated when 1) the simulator ran out of available travel, 2) a number of cycles of an oscillation occurred, or 3) it became evident that a PIO would not occur. Problem variables included presence or absence of motion cues, stick force gradient, pitch attitude visual cue, and the final level of $1/T_{\theta_2}$.

The linear vehicle pitch dynamics used were representative of contemporary fighter-type aircraft and were acceptable to the pilot from a handling-qualities point of view. With reference to the conventional maps of desired short-period characteristics, the simulated aircraft exhibited a stick-fixed natural frequency of 3.0 rad/sec and a damping ratio of 0.5. A consistent set of aerodynamic characteristics was used in the pitch representation, i.e., no artificial relationships existed between pitch transfer function numerator and denominator during normal tracking periods of the experiment. Linear control system dynamics were reduced to those representative of a spring-mass feel system. To examine the effects on PIO behavior due to variations in initial static force gain of the control system, two gradient levels of 6 and 20 lb/in. of stick deflection were selected. The dynamics of the control system afforded a frequency separation by a factor of at least 7 from the stick-fixed short period. Although stick-free bobweight effects were not desired, some were present because of the control stick geometry.

Qualified jet fighter pilots, including individuals of the U. S. Air Force Experimental Test Pilots' School, were used as subjects. No attempt was made to conceal the fact that the tests were concerned with PIO. No special instructions were given with respect to piloting technique. All subjects underwent repeated familiarization tracking exercises in the simulator. This was required to stabilize pre-PIO run-to-run performances. A constant level of tracking performance was desired for individual pilots as an indication that learning was not a pronounced factor in the PIO situation. Measurements of accumulated pitch, attitude, error, and stick motion for pre-PIO tracking with constant airframe-control dynamics were used to evaluate this factor.

Pilot dynamics relative to the stick-force characteristics of the simulated vehicle were a desired output of the analysis. In particular, such data are desired to shed more light on the qualitative observation that pilot force outputs may be dominant in PIO studies. This observation derives from past non-PIO experimental experience, which indicates displacement outputs to be dominant for spring-restrained control sticks when large or preprogramed stick motions are required, and force outputs to be dominant when fine motions and precision control are needed. Previous analyses of specific aircraft systems where PIO occurred[1] indicate that either force or position outputs could be dominant depending on the situation and the nonlinearities present.

The Simulation

Vehicle Representation

Linear two-degree-of-freedom pitch transfer functions were mechanized on an analog computer for pitch and vertical translation. In short-period form, the airframe pitch transfer function was

$$\frac{\theta}{\delta_H} = \frac{K_{\theta_{sp}}(s + 1/T_{\theta 2})}{s[(s/\omega_{sp})^2 + 2\zeta_{sp}s/\omega_{sp} + 1]}$$

with

$$K_{\theta sp} = 2.89 \text{ deg}\theta/\text{deg}\delta_H \qquad 1/T_{\theta 2} = 1.75/\text{sec}$$

$$\omega_{sp} = 3.0 \text{ rad/sec} \qquad \zeta_{sp} = 0.5$$

Vertical velocity was expressed as

$$\frac{w}{\delta_H} = \frac{K_{wsp}\, s + 1/T_{w1}}{(s/\omega_{sp})^2 + 2\zeta_{sp}s/\omega_{sp} + 1}$$

with

$$K_{w_{sp}} = 0.356 \text{ ft/deg}\delta_H \qquad 1/T_{w_1} = 80/\text{sec}$$

A disturbance was applied to the airframe through the following gust-response transfer functions:

$$\frac{\theta}{w_g} = \frac{0.0727}{(s/\omega_{sp})^2 + 2\zeta_{sp}s/\omega_{sp} + 1} \quad \text{deg/fps}$$

$$\frac{w}{w_g} = \frac{0.222\,(s + 4.5)}{(s/\omega_{sp})^2 + 2\zeta_{sp}s/\omega_{sp} + 1} \quad \text{fps/fps}$$

To facilitate analysis, the random-appearing disturbance input chosen to provide a gusting environment simulation was comprised of ten superimposed sine waves of known frequency and amplitude. These forcing functions had been prerecorded on magnetic tape in a 30-min nonrepeating run and were introduced to the airframe in this form. Because the flight task was compensatory, it was necessary to avoid sources of long-term simulator drift; therefore, a first-order high-pass filter was used between the disturbance and airframe to suppress low frequency content. Before the filter was introduced to the analog mechanization, it was nearly impossible to fly the simulator without drifting into its physical stops. After the filter insertion, the simulation experiment was flyable and the pilots reported that the ride was very realistic.

In the analog mechanization used for the airframe, the θ/δ_H and w/δ_H transfer functions are combined to produce normal load factors computed for the aircraft center of gravity and pilot locations; therefore, variations in the pitch transfer function numerator term $1/T_{\theta 2}$ will alter the stick force and deflection per degree of pitch attitude, as well as the stick deflection and force per g. In the course of triggering a PIO during any experimental run, the airframe gain, control system gain, and the airframe short period and damping were all left unaltered, but the increased $1/T_{\theta_2}$ decreased the stick force and deflection per g. Verification of the dynamic characteristics of the analog-mechanized vehicle transfer functions was obtained by a frequency response checkout prior to the experiments.

Control System

The control system available for this set of experiments was physically constructed from a conventional control stick and mechanical spring device. Control system dynamic characteristics were of the form:

$$\frac{\delta_s}{F_p} = \frac{7.13}{s^2 + 1.479(K_F s)^{1/2} + 85.5\,K_F} \quad \text{ft/lb}$$

$$\delta_H/\delta_s = 0.5 \text{ deg/in.}$$

where $K_F \cong 6$ and 20 lb/in.

The transfer function was derived from a measured moment of inertia for the control stick assembly (0.55 slug-ft^2), a measured moment arm of 1.98 ft from the pivot to stick grip, and a damping ratio of 0.08 extracted from time histories of the installed system response to an impulse. Damping was afforded by internal spring friction and bearing friction.

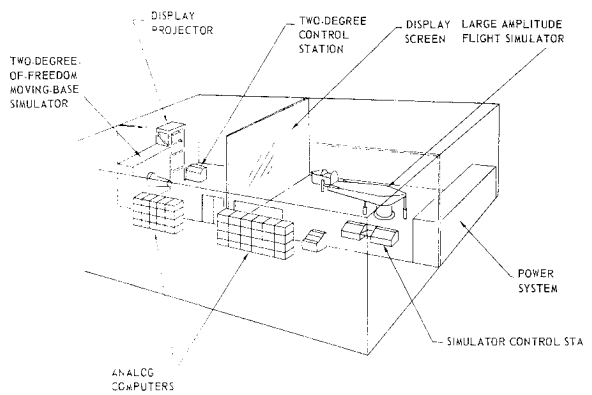

Fig. 2 Flight simulator laboratory.

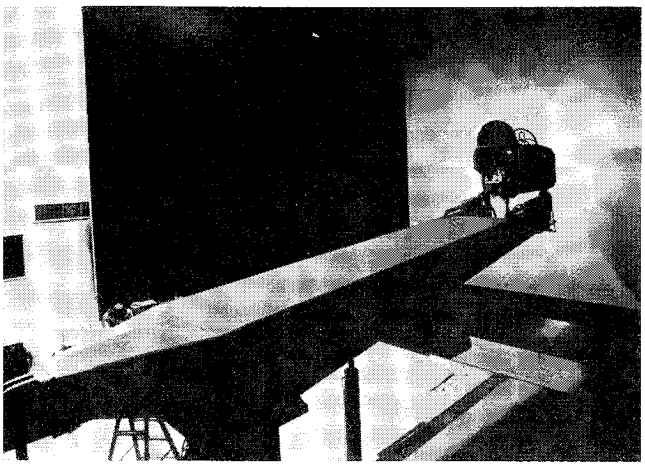

Fig. 3 Large amplitude flight simulator.

It was desired that the static control system characteristics be as linear as possible for a physical spring-stick arrangement. Values of 6 and 20 lb/in. were selected to provide one low gradient typical of contemporary aircraft systems and one high gradient for comparative purposes. The system exhibited very little hysterises (<0.8 lb) for both gradients. Breakout forces were approximately 0.9 lb for the low gradient and almost nonexistent for the heavier gradient. Force at the grip was sensed by a stick-mounted strain gage; stick position was the output of a pivot-mounted potentiometer.

Following installation in the simulator, the control system was found to exhibit stick-free bobweight characteristics. A frequency response of the complete simulator provides data for obtaining these characteristics. Experimental measurements with the heavier gradient yielded deflection and force values of 0.075 in./g and 1.5 lb/g, respectively; for the lighter gradient 0.25 in./g. These values were used in subsequent analyses.

Although stick force data were available for all experiments, it was filtered prior to recording. Dynamics of the filter remained in question during data analysis, so no force related pilot dynamics are included. No similar difficulties were encountered in the collection of stick deflection data. Differences in pilot dynamics relative to displacement characteristics are noted and indicated for the two levels of stick force gradients used in the experiments.

Flight Simulator

The general physical arrangement of the Northrop large amplitude flight simulator and analog computer complex can be discerned from Figs. 2 and 3. Cockpit internal display mockup and arrangement were typical of a contemporary fighter. The only operating flight information available from the internal display was vertical load factor.

As previously stated, the desired simulator flight task was pure compensatory tracking. From a visual cue standpoint, this required that the pilot not be aware of additional pitch attitude cues within the usable cockpit travel of the simulator room other than those being displayed to him on the screen. Physically this is accomplished with a light-absorbing black paint, which surrounds the display screen at the edges of the pilot's peripheral horizontal field. As measured from the pilot's eye, the horizon display nominally occupies 145° of this field. In order that the pilot control only those vehicle dynamics designed in the experiment, it was necessary to avoid simulator electrical and mechanical "washouts" within the region of allowable simulator motion. This required that the analog computer, the simulator and display drives, and the airframe disturbances all be mechan-

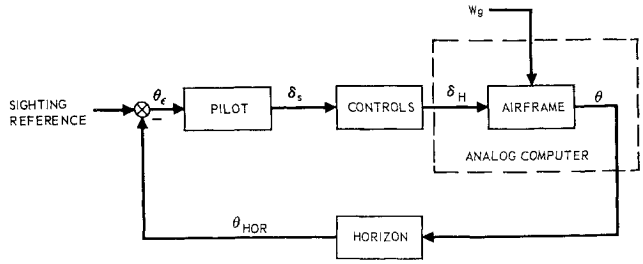

Fig. 4 Fixed-base block diagram.

ized to avoid long term drifts. It was finally possible, by careful experiment design and execution, to cause the pilot always to "fly" the simulator within its physical travel limits without resorting to electrical neutral-seeking washouts.

The flight simulator cockpit was free to translate and rotate in the vertical plane during moving-base experiments. During fixed-base runs the cockpit was held fixed and only the horizon was displaced in response to pitch commands. As previously indicated, roll and directional degrees of freedom were not included in the simulation. General simplified block diagrams covering both the fixed- and moving-base cases are included in Figs. 4 and 5.

The previous discussions were not intended to imply the absence of significant dynamics due to the simulator motion systems. In fact, the production of full-scale load factors and motion cues required a more precise definition of system dynamics than was available at the outset of the experimental design period. Successive simulator response tests provided this definition; some of the more pertinent system dynamics are revealed in Fig. 6.

Discussion of Results

From linear systems analysis theory it has been postulated that, following PIO onset, the nearly sinusoidal sustained motion gives rise to a simple gain-pilot-describing function.[1] The theory further assumes primary pilot response is to visual pitch-attitude cues. Under such conditions a linear PIO could be predicted to occur if the value of $2\zeta_{sp}\omega_{sp} - 1/T_{\theta_2}$ could become negative. Physically, an unusual airplane configuration would be required to make this value negative. Using the approximate factors of Ref. 5,

$$2\zeta_{sp}\omega_{sp} - 1/T_{\theta_2} \cong -M_q - M_{\dot{\alpha}} - (Z_\delta/M_\delta)M_w$$

where $-M_\delta/Z_\delta$ is proportional to the effective elevator control arm (measured positive forward). To make the right side of this equation negative would require a canard configuration (positive control arm and negative M_w) or a low value of $-M_q$ and a small control arm. Without belaboring this point further, it appears that imposing such dynamics might be used as an expedient to produce conditions of PIO

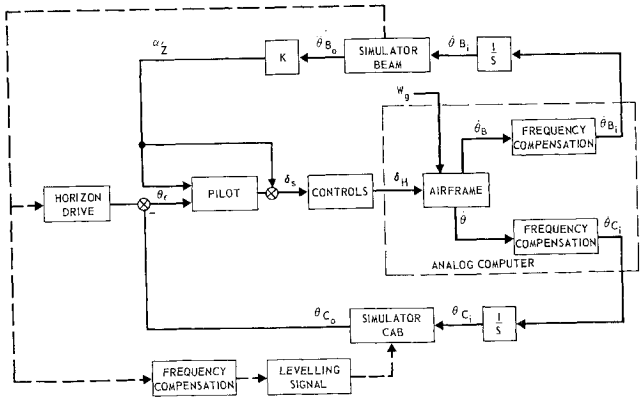

Fig. 5 Moving-base block diagram.

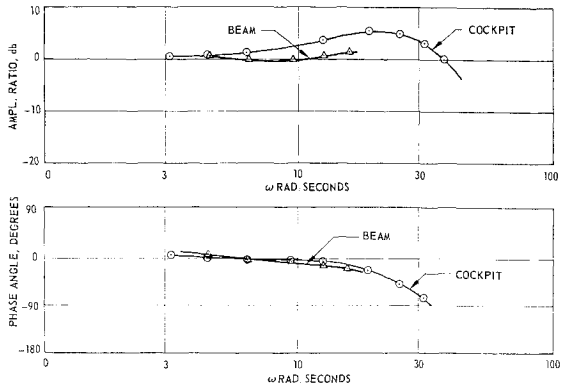

Fig. 6 Simulator frequency response.

and examine the pilot behavior in more detail. Such an approach was elected in this series of ground-based simulator experiments.

Of first significance is the fact that PIO's were generated under both fixed-base (θ cues only) and moving-base conditions as a result of sudden changes in $1/T_{\theta_2}$ from the original level (1.75) to elevated levels. Assuming a synchronous gain "pilot" and no control system dynamics, an increase in $1/T_{\theta 2}$ to 3.0 would result in a theoretical pitch attitude locus asymptotic to the imaginary axis. Values in excess of this would theoretically give rise to PIO if the increase occurred rapidly enough to preclude significant initial pilot gain adaptation. This is illustrated in the root locus plots of Figs. 7 and 8. The control system dynamics are included in these loci. Although control system effects are small at the PIO frequencies, the $1/T_{\theta_2} = 3.0$ locus now crosses the imaginary axis. It can be seen that a reduction in pilot gain could prevent a pure gain-pilot from getting into a PIO situation at the values of $1/T_{\theta_2}$ shown; hence, $1/T_{\theta_2}$ was increased very rapidly in the experiments. Also, any other pilot adaptation would result in different loci from those shown.

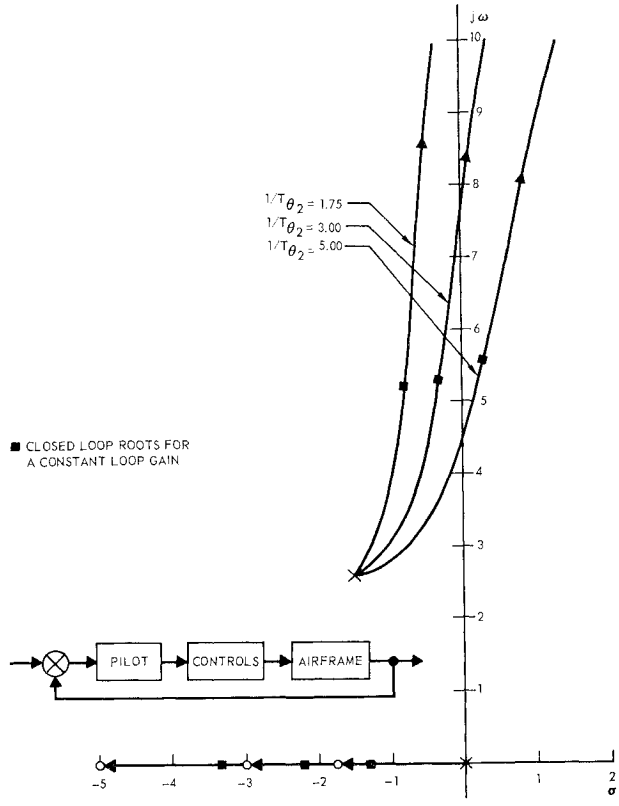

Fig. 7 Root locus plot with low stick force gradient.

Table 1 Moving-base runs

$w_{g_{rms}}$, fps	$1/T_{\theta_2}$, 1/sec	ω, rad/sec	δ_s/a'_z Phase, deg (lag)	δ_s/a'_z A.R., in./g	δ_s/θ_2 Phase, deg	δ_s/θ_2 A.R., in./deg	Remarks
			Low stick-force gradient				
10	3.46	4.16	68	0.69	25 lag	0.15	9 cycles, decreasing amplitude
10	3.75	3.60	98	0.58	54 lag	0.25	5 cycles, increasing amplitude
6	2.90	3.96	79	0.75	50 lag	0.24	5½ cycles, increasing amplitude
10	3.46	3.41	78	0.34	36 lead	0.18	2½ cycles, constant amplitude
10	3.00	5.50	56	3.25	7 lead	2.66	3 cycles, increasing amplitude
10	2.71	5.50	60	2.55	7 lead	3.24	3 cycles, increasing amplitude
6	3.29	5.61	29	2.45	56 lead	1.36	4½ cycles, constant amplitude
10	3.00	5.15	63	1.95	46 lead	1.51	6 cycles, increasing amplitude
8	3.46	4.04	59	0.95	49 lead	0.42	3 ½ cycles, decreasing amplitude
10	3.46	3.34	79	0.52	35 lead	0.30	7 cycles, constant amplitude
10	3.48	4.12	60	0.48	29 lead	0.32	8 cycles, constant amplitude
10	3.46	4.12	48	0.86	29 lead	0.37	8 cycles, constant amplitude
			High stick-force gradient				
8	3.00	3.99	75	1.35	24 lag	0.95	3 cycles, constant amplitude
...	3.10	3.63	68	0.79	10 lag	0.46	2 ½ cycles, constant amplitude
16	4.06	3.63	74	0.54	31 lead	0.39	4 cycles, constant amplitude
6	3.90	3.80	63	0.88	32 lead	0.40	5 cycles, constant amplitude
10	3.46	4.00	66	0.88	54 lead	1.31	4 cycles, decreasing amplitude
10	4.25	4.12	50	0.72	39 lead	0.48	6 cycles, decreasing amplitude
6	3.29	4.75	33	1.35	57 lead	...	14 cycles, increasing amplitude
6	3.29	4.68	44	3.59	27 lead	1.53	5 cycles, increasing amplitude
10	3.29	4.12	52	1.15	37 lead	0.55	4 cycles, decreasing amplitude
10	2.71	4.12	40	1.59	5 lead	0.83	7½ cycles, constant amplitude

This could account for the fact that PIO's may not occur at exactly the frequencies that these loci would predict.

Several of the runs in which a PIO existed are tabulated in Table 1 (moving-base runs) and Table 2 (fixed-base runs). Listed are the average PIO oscillation frequency, the level of the disturbance input, the final value of $1/T_{\theta_2}$, and the phase and amplitude ratio of δ_s/a'_z and δ_s/θ_c. Under fixed-base conditions, an increase to approximately 17.0 was necessary to produce an oscillation. A single case of fixed-base PIO was noted for a $1/T_{\theta_2}$ of 8.5. The graphically observed closed-loop oscillation frequency was not closely related to the final value of $1/T_{\theta_2}$. This frequency because of the graphical method of data reduction represents an average frequency over the oscillation. Portions of the time histories of a typical run are reproduced in Figs. 9 and 10, both before and after the PIO.

The vital nature of load factor cues was indicated by pilot comment. One pilot, to help prevent overcontrolling, steadied his right arm with his right leg and also on occasion with his left hand. Two of the pilots, both with extensive flight experience in PIO situations, used an unconventional open grip on the stick. This technique prevented any possible application of force on the stick in an unintended direction. These techniques would seem to reduce any limb-manipulator coupling.

During some of the actual PIO's, the simulator beam motion reached a rate limit. The effect of this limit was to cause vertical load factor experienced at the cockpit to approach a triangular waveform instead of the expected sinusoid. The effect of this characteristic on pilot dynamic behavior could not be isolated in the analysis; however, on being questioned, the pilots did not seem to be aware of the difference in motion cue.

A brief investigation of the effect of $1/T_{\theta_2}$ at values below the nominal value of 1.75 was conducted. One run was made moving-base and one fixed-base. A disturbance was used in both cases. No quantitative analysis was made but pilot comment indicated that there was a loss of control as $1/T_{\theta_2}$ was reduced. During the moving-base run the pilot was aware that more stick was required when $1/T_{\theta_2}$ reached 1.15; at 0.75 he noted a further loss of control, at 0.40 he stated that he was "really tugging" on the stick, and at 0.20 he was "riding—that's all." During the fixed-base run, a slight loss in control was noted as $1/T_{\theta_2}$ was reduced from

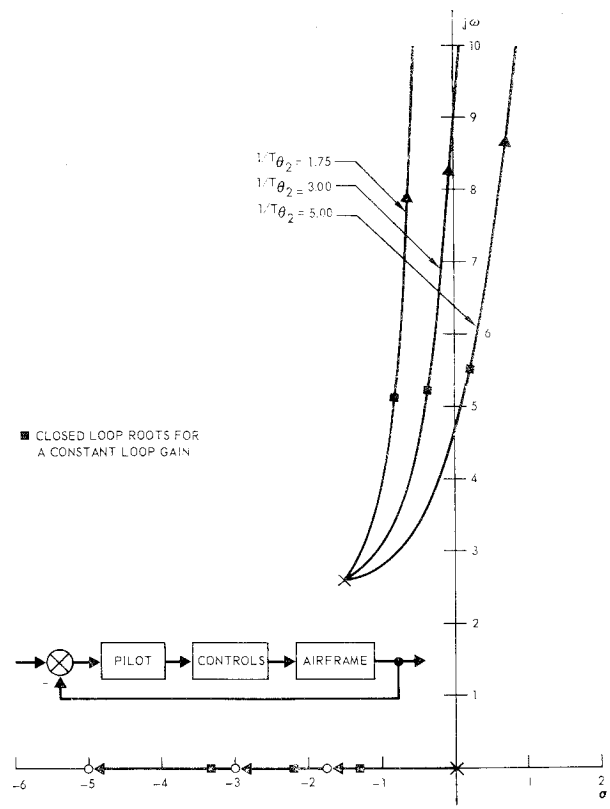

Fig. 8 Root locus plot with high stick force gradient.

Table 2 Fixed-base runs

w_{grms}, fps	$1/T_{\theta_2}$, 1/sec	ω, rad/sec	δ_s/a'_z [a] Phase, deg (lag)	δ_s/a'_z [a] A.R., in./g	$\delta_s/\theta\epsilon$ Phase, deg (lead)	$\delta_s/\theta\epsilon$ A.R., in./deg	Remarks
			Low stick-force gradient				
10	8.48	4.12	84	0.49	36	0.56	3 cycles, decreasing amplitude
10	19.05	4.12	90	0.20	0	0.18	2½ cycles, decreasing amplitude
10	20.95	3.64	85	0.11	0	0.16	2 cycles, constant amplitude
10	40.25	3.99	70	0.067	15	0.098	6 cycles, decreasing amplitude
10	30.55	4.12	79	0.11	0	0.14	3 cycles, decreasing amplitude
10	16.95	4.58	48	0.43	33	0.54	6½ cycles, decreasing amplitude
6	18.05	4.85	65	0.43	25	0.57	5 cycles, constant amplitude
10	19.05	4.26	42	0.29	6	0.37	9½ cycles, decreasing amplitude
10	19.05	4.12	48	0.16	43	0.31	9 cycles, decreasing amplitude
10	16.95	4.12	60	0.19	8	0.26	4 cycles, decreasing amplitude
			High stick-force gradient				
8	30.55	4.50	44	0.23	30	0.23	2 cycles, decreasing amplitude
6	18.05	4.86	44	0.14	50	0.58	8½ cycles, decreasing amplitude
10	16.95	4.98	44	0.38	36	0.46	9 cycles, constant amplitude
10	24.85	4.26	65	0.27	21	0.21	7 cycles, decreasing amplitude

[a] Listed for reference only using computed normal acceleration. In the fixed-base mode, of course, no accelerations were developed.

1.75 down to 0.20. At 0.10 the pilot noted that larger stick movements were required but that damping had remained constant. With $1/T_{\theta_2}$ reduced to zero he could not prevent large horizon excursions.

Conclusions

Certainly a good deal of spread can be observed in the data; scatter seems inevitable with human subjects and learning on the part of the pilots probably never ceased. However, the sum of this experience suggests several vital points about the effective pilot dynamics occurring during PIO.

1) With only the visual cue available during an oscillation, the pilot does not appear to operate in a purely synchronous manner unless it is possible that he is capable of almost instantaneous large magnitude gain adaptation. Adaptation of this nature would be required for a synchronous pilot to avoid a PIO at the level of $1/T_{\theta_2}$ used. Based on previous human response research,[1] such adaptation does not seem feasible.

2) When a pilot flies a visual loop with full-scale motion cues available to him, his dynamics are altered from the motionless pure visual case. The availability of full-scale motion cues causes the pilot model to appear more synchronous in the visual loop; however, the same data more consistently show the pilot operating with lag dynamics on the load factor cues.

3) In regard to the two stick-force spring gradients used, the high gradient generally appeared to reduce PIO tendencies. However, some PIOs were generated with each spring at about the same values of $1/T_{\theta_2}$.

4) Under both moving- and fixed-base conditions, a reduction in $1/T_{\theta_2}$ to values near zero produced a situation of inferior controllability and worsened pilot opinion.

The reader is cautioned that the suggested PIO pilot dynamics are stationary descriptions, and as such are valid during PIO, but not during the transition period to PIO from a previously stable behavior. Further, it is emphasized that the tests provide discrete frequency points, not a continuous frequency domain.

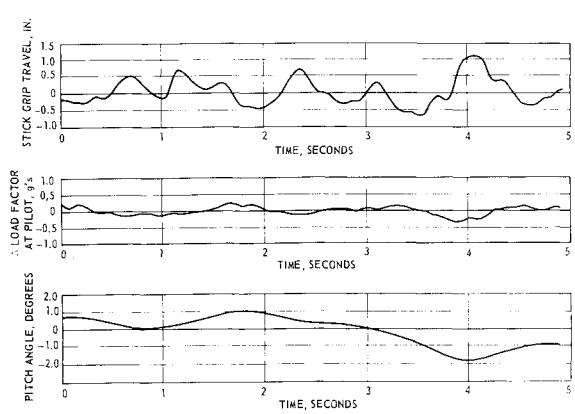

Fig. 9 Pre-PIO tracking time history, moving-base.

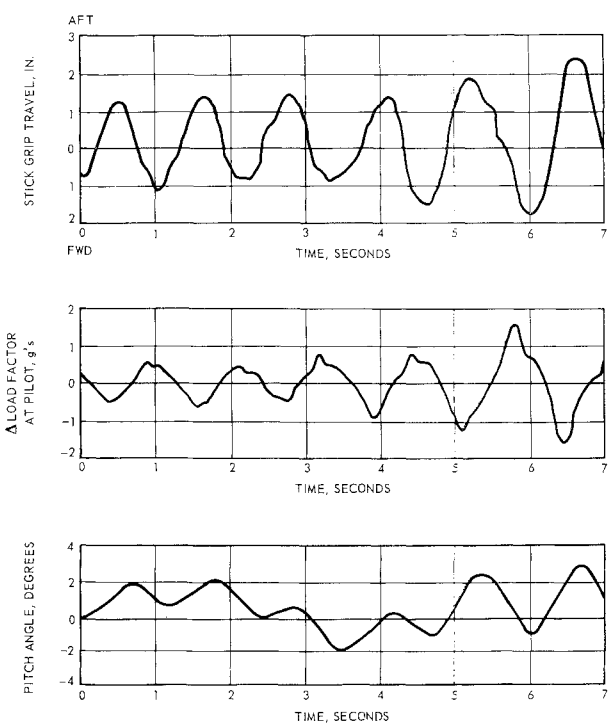

Fig. 10 Typical PIO time history, moving-base.

References

[1] Ashkenas, I. L., Jex, H. R., and McRuer, D. T., "Pilot-induced oscillations: Their cause and analysis," Northrop Corp., Norair Div., Rept. NOR-64-143 (1964); also Systems Technology Inc., Rept. TR-239-2 (June 20, 1964).

[2] Ashkenas, I. L., "Comment on 'Low-altitude, high-speed handling and riding of volities,' " J. Aircraft **1**, 222–223 (1964); also A'Harrah, R. C., "Reply by author to I. L. Ashkenas," J. Aircraft **1**, 223–224 (1964).

[3] Hirsch, D. L., "Investigation and elimination of PIO tendencies in the Northrop T-38A," Society of Automotive Engineers (July 1964).

[4] Levi, O. A. and Nelson, W. E., "An analytical and flight test approach to the reduction of pilot induced oscillation susceptibility," *AIAA/AFFTC/NASA-FTC Testing of Manned Flight Systems* (American Institute of Aeronautics and Astronautics, New York, 1963), pp. 1–9; also J. Aircraft **1**, 178–184 (1964).

[5] Ashkenas, I. L., and McRuer, D. T., "Optimization of the flight-control, airframe system," J. Aerospace Sci. **27**, 197–218 (1960).

NOV.-DEC. 1966 J. AIRCRAFT VOL. 3, NO. 6

Recent Research Results in the Aerodynamics of Supersonic Vehicles

A. Warner Robins,* Odell A. Morris,† and Roy V. Harris Jr.‡
NASA Langley Research Center, Hampton, Va.

The continuing aerodynamic-research effort aimed at improving the design of supersonic-cruise vehicles has recently produced some significant results. Research by both government and industry has provided, in addition to a better understanding of the design problem itself, some new and very useful design tools and concepts. Some of the advantages of these methods in the treatment of wave drag and drag due to lift are briefly discussed. Also presented are some new considerations of aerodynamic interference and its effect on the aerodynamic efficiency of the trimmed vehicle. An illustrative example of the application of these design tools and concepts to the aerodynamic design of a supersonic-cruise vehicle (SCAT 15-F) is made. A parallel analytic and experimental buildup of the vehicle is presented, including treatment of the symmetric (flat camber-plane), the warped, and the warped-and-reflexed versions of the configuration. The potential of the new techniques is demonstrated by the good agreement between experiment and theory and by the high level of vehicle performance.

Introduction

A BASIC aim of aerodynamic research is to provide the design aerodynamicist with rational, rapid, and reliable means for evaluating the aerodynamics of a given aerodynamic shape and to enable him to assess quickly the cost in aerodynamic efficiency of proposed changes in vehicle shape brought about by other considerations. A short reaction time for the aerodynamicist will permit him to participate more effectively at the vehicle concept stage and thus provide for a more comprehensive design process. Intensive effort by both government and industry therefore has been devoted to the implementation of existing theory with new analytical numerical methods such that the high-speed computer might provide calculative results heretofore restricted to certain relatively simple shapes. Some significant contributions to this end have recently been made. These, along with other new considerations of the aerodynamics of the supersonic vehicle, will be discussed.

Presented as Preprint 65-717 at the AIAA/RAeS/JSASS Design and Technology Meeting, Los Angeles, Calif., November 15–18, 1965; submitted January 13, 1966; revision received June 22, 1966.

* Head, Supersonic Mechanics Section, Full Scale Research Division.

† Aerospace Engineer, Full Scale Research Division.

‡ Aerospace Engineer, Full Scale Research Division. Member AIAA.

Discussion

Zero-Lift Wave Drag

One of the most useful developments has been the application of the high-speed computer to the problem of rapidly determining the zero-lift wave drags of highly complex shapes. Most early efforts aimed at treating the complex case, such as the "transfer rule" of Ward[1] and, of course, supersonic area rule,[2, 3] involved the concept of equivalent bodies of revolution. These efforts had depended upon graphical or semigraphical schemes for generation of the geometry of the many equivalent bodies and utilized, with erratic results, a Fourier series representation of the slopes of areas of these bodies in the drag calculations. More recent schemes[4] accomplish the geometric exercise with the computer using a mathematical model of the aircraft as shown in Fig. 1 and determine the drag of the equivalent bodies as represented by least-drag paths through the computed cross-sectional areas. The result is a significant advancement in both speed and accuracy. The right-hand portion of the figure shows the agreement between calculated and experimental values in the Mach number range from 1.4 to 3.2 for very complex, complete configurations designed for supersonic cruise, varying from fighter-type vehicles on the upper right to bomber and transport types on the left. Except for the three high points, all of which may have resulted from boundary-layer separation, the agreement is generally good. Such computer programs certainly represent a powerful aid to the design aerodynamicist.